Acta Pharmaceutica Sinica B 2025;15(2):1070−1083

Chinese Pharmaceutical Association
Institute of Materia Medica, Chinese Academy of Medical Sciences

Acta Pharmaceutica Sinica B

www.elsevier.com/locate/apsb
www.sciencedirect.com

ORIGINAL ARTICLE

A novel anti-ischemic stroke candidate drug AAPB with dual effects of neuroprotection and cerebral blood flow improvement

Jianbing Wu[a,†], Duorui Ji[a,†], Weijie Jiao[a,b], Jian Jia[a,c], Jiayi Zhu[a], Taijun Hang[d], Xijing Chen[e], Yang Ding[f], Yuwen Xu[g], Xinglong Chang[h], Liang Li[h], Qiu Liu[h], Yumei Cao[h], Yan Zhong[h], Xia Sun[h], Qingming Guo[h], Tuanjie Wang[h], Zhenzhong Wang[h], Ya Ling[h], Wei Xiao[h,i,*], Zhangjian Huang[a,*], Yihua Zhang[a,*]

[a]*State Key Laboratory of Natural Medicines, Jiangsu Key Laboratory of Drug Discovery for Metabolic Diseases, Center of Drug Discovery, China Pharmaceutical University, Nanjing 210009, China*
[b]*Department of Pharmacy, Henan Province Hospital of Traditional Chinese Medicine, the Second Affiliated Hospital of Henan University of Chinese Medicine, Zhengzhou 450002, China*
[c]*Novel Technology Center of Pharmaceutical Chemistry, Shanghai Institute of Pharmaceutical Industry Co., Ltd., China State Institute of Pharmaceutical Industry, Shanghai 201203, China*
[d]*Department of Pharmaceutical Analysis, China Pharmaceutical University, Nanjing 210009, China*
[e]*Clinical Pharmacokinetics Laboratory, School of Basic Medicine and Clinical Pharmacy, China Pharmaceutical University, Nanjing 211198, China*
[f]*Key Laboratory of Drug Quality Control and Pharmacovigilance (Ministry of Education), State Key Laboratory of Natural Medicines, Department of Pharmaceutics, China Pharmaceutical University, Nanjing 210009, China*
[g]*Crystal Pharmatech Co., Ltd., Suzhou 215123, China*
[h]*State Key Laboratory on Technologies for Chinese Medicine Pharmaceutical Process Control and Intelligent Manufacture, Jiangsu Kanion Pharmaceutical Co., Ltd., Lianyungang 222001, China*
[i]*Nanjing University of Chinese Medicine, Nanjing 210023, China*

Received 22 September 2024; received in revised form 25 November 2024; accepted 18 December 2024

*Corresponding authors.
E-mail addresses: xw_kanion@163.com (Wei Xiao), zhangjianhuang@cpu.edu.cn (Zhangjian Huang), zyhtgd@163.com (Yihua Zhang).
[†]These authors made equal contributions to this work.
Peer review under the responsibility of Chinese Pharmaceutical Association and Institute of Materia Medica, Chinese Academy of Medical Sciences.

https://doi.org/10.1016/j.apsb.2024.12.042

KEY WORDS

Ischemic stroke;
Nitric oxide;
AAPB;
Neuroprotection;
Blood flow improvement;
Dual effects;
Safety profiles;
Pharmacokinetic properties

Abstract Ischemic stroke (IS) is a globally life-threatening disease. Presently, few therapeutic medicines are available for treating IS, and rt-PA is the only drug approved by the US Food and Drug Administration (FDA) in the US. In fact, many agents showing excellent neuroprotection but no blood flow-improving activity in animals have not achieved ideal clinical efficacy, while thrombolytic drugs only improving blood flow without neuroprotection have limited their wider application. To address these challenges and meet the huge unmet clinical need, we have designed and identified a novel compound AAPB with dual effects of neuroprotection and cerebral blood flow improvement. AAPB significantly reduced cerebral infarction and neural function deficit in tMCAO rats, pMCAO rats, and IS rhesus monkeys, as well as displayed exceptional safety profiles and excellent pharmacokinetic properties in rats and dogs. AAPB has now entered phase I of clinical trials fighting IS in China.

1. Introduction

Ischemic Stroke (IS) is a severe cerebrovascular disease, associated with significantly high morbidity and mortality worldwide[1]. Multiple strategies have been adopted to reconstruct the blood supply to the brain, and the two mainstays are intravenous thrombolysis and endovascular thrombectomy, which can realize brain vessel recanalization by chemically dissolving and mechanically retrieving a clot, respectively. However, the therapeutic time window of thrombolysis (≤4.5 h) or mechanical thrombectomy (≤6 h) is narrow, and often with the risk of hemorrhagic transformation[2,3]. In addition, due to multiple contraindications, only a few IS patients have received thrombolysis, and about 50% of them can be fully recovered[4]. The mechanical thrombectomy is limited to the treatment of patients' basilar artery occlusion in hospitals with relatively qualified conditions[5]. In view of that both thrombolysis and thrombectomy cannot generate neuroprotection and display limited clinical application, researchers have recently explored the combination therapy of vascular recanalization with neuroprotective drugs/agents against IS, and achieved good results[6-12].

Given the necessity of drug therapy for patients who are illegible to undergo thrombolysis or thrombectomy, and the efficacy of drug(s) in assisting vascular recanalization, the utilization of drugs should occupy an important position against IS. Unfortunately, only few small molecule drugs such as *R*,*S*-3-*n*-butylphthalide (NBP) and edaravone (Eda) are presently employed for the treatment of IS, thus an urgent and huge unmet clinical need exists[13].

The mechanism of brain injury caused by IS involves excitotoxicity, inflammation, oxidative/nitrosative stresses, apoptosis and so on[14]. And the one-drug and/or one-target therapeutic

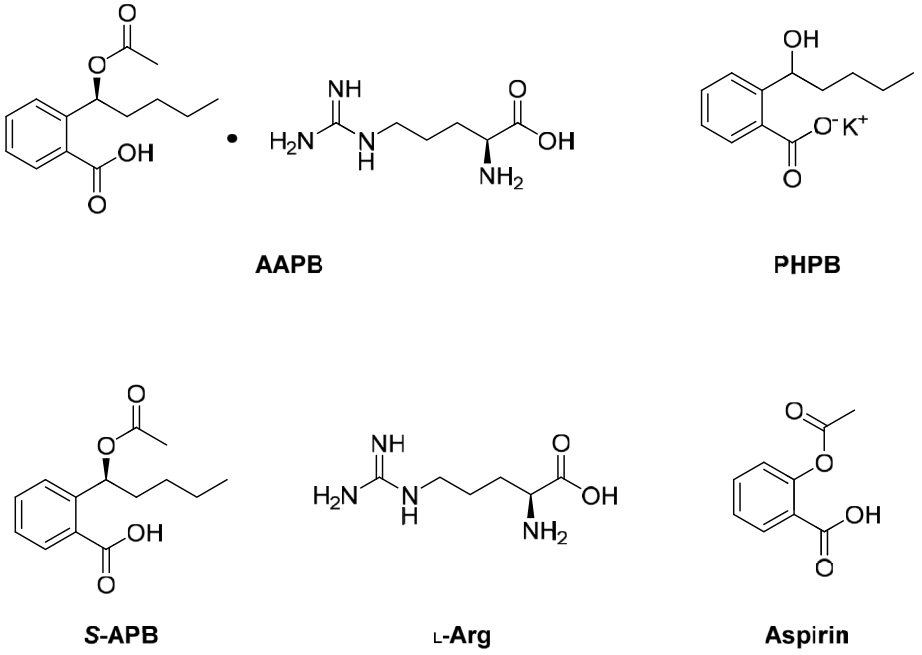

Figure 1 The structures of AAPB, PHPB, *S*-APB, L-Arg and Aspirin.

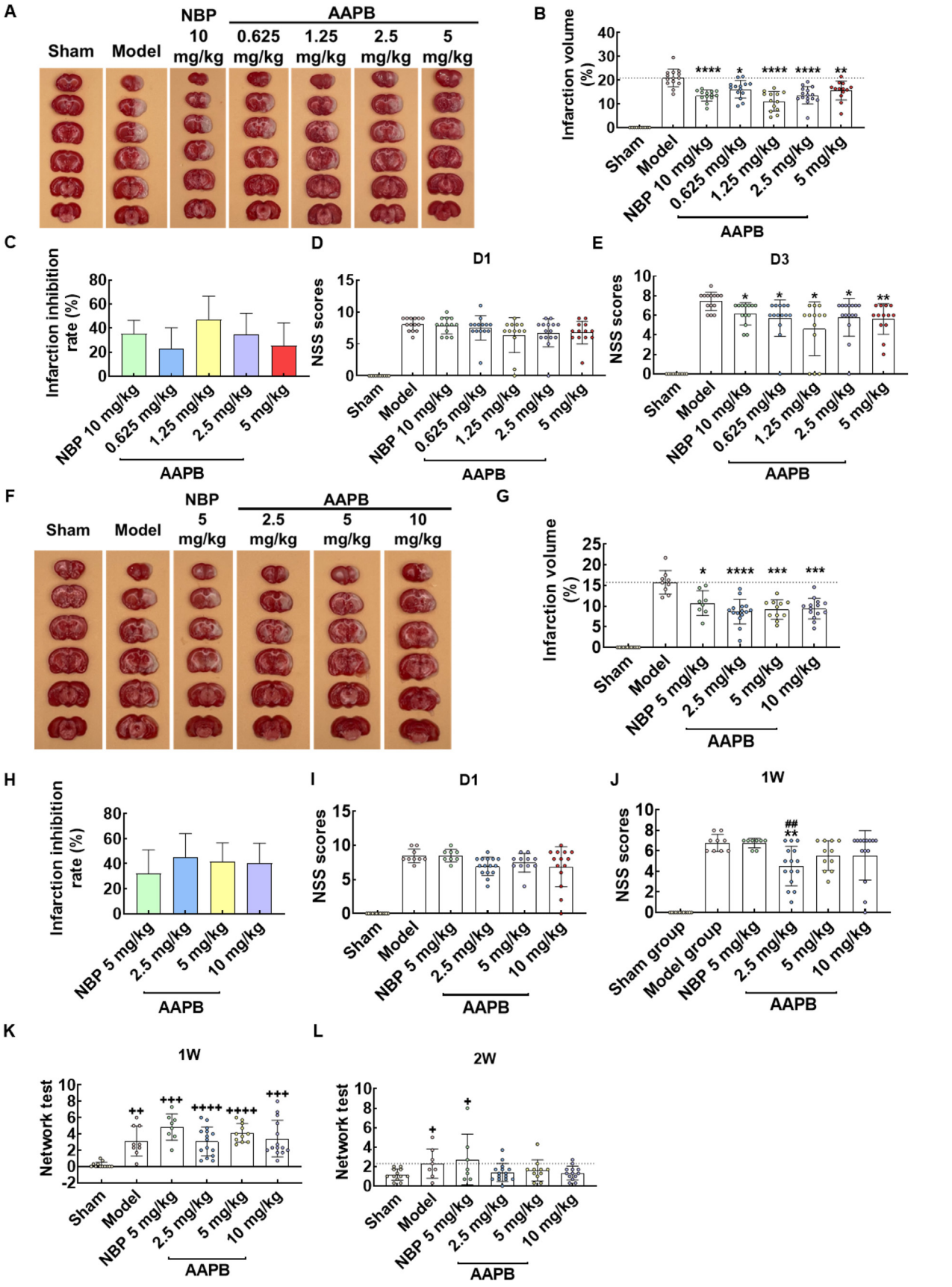

Figure 2 AAPB treatment reduced infarct volume and improved neurologic function in rat models of acute (A−E) and chronic (F−L) IS. (A) Representative picture of TTC staining. (B, C) Quantification of the infarct volume (%) and inhibition ratio (%). (D, E) NSS values at days 1 and 3 after surgery. (F) Representative picture of TTC staining. (G, H) Quantification of the infarct volume (%) and inhibition ratio (%). (I, J) NSS

strategy has become increasingly inefficient. Therefore, discovery of new anti-IS drugs, especially those targeting multiple pathways, holds great scientific significance and practical value[15].

For a long time, most anti-IS drug studies focused on neuroprotection and neglected the integrity of brain function and the interactions of different portions of the brain. In view of this, Lo et al. proposed a concept of the neurovascular unit (NVU), aiming to emphasize the importance of interactions and mutual influences of different cerebral components[16-18]. Since then, the research on anti-IS drugs has gradually shifted from solely neuroprotection to both neuroprotection and vascular protection.

Many agents like nerinetide (NA-1) showing excellent neuroprotection but no blood flow improvement in animals have failed to achieve desirable clinical efficacy[19,20], and the thrombolytic drugs like the recombinant tissue plasminogen activator (rt-PA) simply improving blood flow without neuroprotection have limited their wider application[21-23]. To address these challenges, and grounded in that the combination of brain vascular recanalization with neuroprotective drugs/agents may improve therapeutic outcomes[6-12], we proposed a scientific hypothesis that an agent with dual effects of neuroprotection and cerebral blood flow improvement may become a promising anti-IS candidate drug.

Some exogenous nitric oxide (NO) donors are known to release NO in the body, dilate cerebral vessels, improve blood supply to brain tissue, and play a significant anti-IS activity[24-27]. Reportedly, L-arginine (L-Arg, Fig. 1) can generate NO by NO synthase (NOS), improve cerebral microcirculation, alleviate acute ischemic injury, and significantly reduce the symptoms and severity of stroke[28-30].

The neuroprotective agent potassium 2-(1-hydroxypentyl)-benzoate (PHPB, Fig. 1) is derived from the ring-opening of the lactone in NBP, with an anti-IS activity comparable to NBP but better physicochemical and pharmacokinetic properties[31-34]. PHPB is currently undergoing phase II-III of clinical trials fighting the acute IS in China.

Aspirin (ASP, Fig. 1), namely *O*-acetoxybenzoic acid, irreversibly acetylates the hydroxyl group of serine at position 530 in cyclooxygenase-1 (COX-1), preventing the conversion of arachidonic acid (AA) to thromboxane A2 (TXA2). ASP is a globally recognized classic anti-thrombotic drug and is widely used in the prevention and treatment of IS, especially in the high-risk patients[35,36].

Keeping these in mind, to verify our hypothesis, based on the NVU concept and employing a multi-target action strategy, we have designed and identified a novel compound, namely L-arginine *S*-2-(1-acetoxy-*n*-pentyl)-benzoate (AAPB, Fig. 1), where the pharmacophore features of three drugs (ASP, PHPB, and L-Arg) are structurally integrated into one molecule, meanwhile, performed a series of preclinical investigations.

2. Results

2.1. AAPB potently inhibits platelet aggregation, coagulation, and thrombosis in cellular or animal models

AAPB significantly inhibited adenosine 5'-diphosphate (ADP)- and AA-induced platelet aggregation *in vitro* with IC_{50} (mmol/L) values of 0.67 ± 0.05 and 0.16 ± 0.02, superior to NBP, *S*-NBP, *S*-APB + L-Arg (two moieties of AAPB), PHPB and ASP, respectively (Supporting Information Table S1).

The anti-coagulation effect of AAPB was assessed by the bleeding time of tail clipping in mice. The bleeding time (min) of AAPB at 5 mg/kg (25.31 ± 1.01) was greater than that of ASP at 5 mg/kg (22.52 ± 1.31) (Supporting Information Table S2).

The anti-thrombotic activity of AAPB was evaluated in an arteriovenous shunt thrombosis model in rats. AAPB (10 mg/kg, i.v.) significantly reduced wet/dry thrombus in rats by 44.14% and 45.02%, more effective than that of *S*-NBP (33.24%, 25.95%), PHPB (15.39%, 11.32%), and ASP (40.74%, 39.67%), at the same dose, respectively (Supporting Information Table S3).

2.2. AAPB displays significant anti-cerebral ischemic and neuroprotective activities in rats and rhesus monkeys

2.2.1. In rat models of acute and chronic IS

In a rat model of acute IS, compared with the model group, NBP (10 mg/kg) reduced the cerebral infarction volume by 35%, while AAPB (0.625, 1.25, 2.5, and 5 mg/kg) decreased that by 23%, 47%, 35% and 25% (Fig. 2A–C), and neurological symptom score (NSS) values in AAPB groups were significantly lower than that in the model group, respectively (Fig. 2D, E).

In a rat model of chronic IS, NBP (5.0 mg/kg) decreased the cerebral infarction volume by 32%, while AAPB (2.5, 5.0 and 10 mg/kg) more significantly reduced that by 45%, 42% and 41%, respectively (Fig. 2F–H). The NSS values of AAPB groups, especially that of 2.5 mg/kg group significantly lower than that in the model or NBP group (Fig. 2I, J).

The grid test showed that at day 14 after modeling, the misstep frequency of rats in the model or NBP group was significantly higher than that in the sham group, while all AAPB groups recovered to the level in the sham group (Fig. 2K, L).

The body weight of AAPB (5.0 or 10 mg/kg) group was significantly higher than that of the model group from day 4 after modeling to the end of the experiment (Supporting Information Fig. S2A). And the survival rate of AAPB (2.5 mg/kg) group was significantly higher than that in the model or NBP group (Fig. S2B and S2C).

2.2.2. In a rat model of permanent IS

NBP (10 mg/kg) group decreased the cerebral infarction volume in rats by 7%, without a statistical difference, compared with the model group, while AAPB (0.625, 1.25 and 2.5 mg/kg) groups substantially inhibited that by 14%, 20% and 12%, and the infarction volume in 0.625 or 1.25 mg/kg group was significantly lower than that in the model group (Fig. 3A–C).

And at day 1 after surgery, the NSS value of NBP group was lower than that of the model group but without significant difference, while NSS values of AAPB groups were significantly lower than that of the model group. On day 3 after surgery, NSS values in AAPB groups were significantly lower than that in the model group, better than NBP (Fig. 3D and E).

2.2.3. In a rhesus monkey model of IS

The cerebral infarction volume in AAPB low (0.6 mg/kg)- or high (1.2 mg/kg)-dose group showed a therapeutic trend on day 5,

values at days 1 and 3 after surgery. (K, L) Misstep frequency of surviving animals at weeks 1 and 2 after surgery. Data are mean ± SD (n = 8 – 15). *$P < 0.05$, **$P < 0.01$, ***$P < 0.001$ and ****$P < 0.0001$, compared to the model group. $^{\#}P < 0.05$ and $^{\#\#}P < 0.01$, compared to the NBP group. $^{+}P < 0.05$, $^{++}P < 0.01$, $^{+++}P < 0.001$ and $^{++++}P < 0.0001$, compared to the sham group.

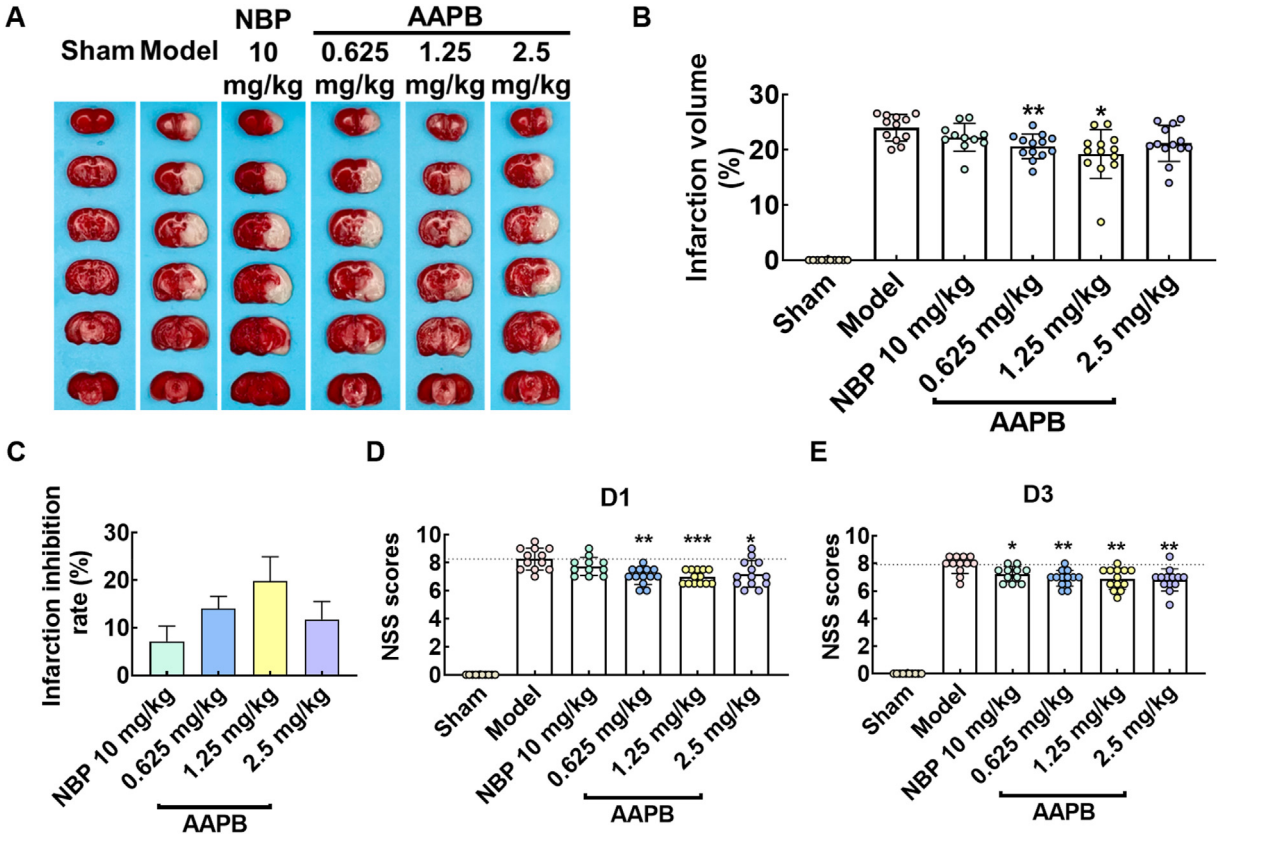

Figure 3 AAPB treatment reduced infarct volume and improved neurologic function in a rat model of permanent IS. (A) Representative picture of TTC staining. (B, C) Quantification of the infarct volume (%) and inhibition ratio (%). (D, E) NSS values at days 1 and 3 after surgery. Data are mean ± SD (n = 10−13). *P < 0.05, **P < 0.01 and ***P < 0.001, compared to the model group.

compared with that at day 2 after modeling. At day 9, the progression percentages of cerebral infarction decreased while the recovery rates increased in AAPB low- or high-dose group. From day 16 after modeling to the end of the experiment, the progression percentages and recovery rates of cerebral infarction in AAPB low- or high-dose group were greatly improved, compared with the model group, and the recovery rates in AAPB low- or high-dose group were dose-dependently increased (Fig. 4A−D).

At each time point, the progression percentage of neurological deficit score (NDS) decreased and the recovery rate of NDS increased in AAPB low- or high-dose group, compared with that in the model group. At days 9, 16, and 23 after modeling, the progression percentages and recovery rates of NDS in AAPB low-dose group were significantly improved, compared with the model group. And the progression percentages at days 9, 16, and 30 and the recovery rate at day 16 of NDS after modeling in AAPB high-dose group were significantly improved, compared with the model group, respectively (Fig. 4E−J).

After modeling, the average foraging frequency and utilization rate of the affected limb in AAPB low- or high-dose group were not significantly decreased, compared with those before modeling, and were significantly higher than those in the model or NBP group at corresponding time points. Compared with the model or NBP group, the foraging time of AAPB low- or high-dose group decreased at each time point, and the single foraging time of AAPB high-dose group was significantly decreased at days 11, 18, 25, and 37 after modeling, compared with that in the model group (Fig. 4K−P).

There were no significant changes in body weight and body temperature of animals in AAPB low- or high-dose groups after operation, compared with those before modeling (Supporting Information Fig. S3). Under the experiment conditions, the effective dose of AAPB was 0.6 mg/kg, more active than NBP at 4.6 mg/kg.

2.2.4. *Therapeutic time window of AAPB in a rat model of acute IS*

AAPB (1.25 mg/kg) administration at 1, 2, 4, 6, and 8 h after ischemia significantly lowered the cerebral infarction volume by 34%, 34%, 35%, 23%, and 16%, measured 24 h after each treatment, respectively (Supporting Information Fig. S4). And the therapeutic time window of AAPB for IS rats was 8 h, and the best therapeutic effect could be achieved within 4 h post ischemia.

2.3. *Studies on the mechanism of action of AAPB in in vitro and in vivo*

2.3.1. *AAPB generates NO and S-nitrosates PTEN (phosphatase and tensin homolog deleted on chromosome ten)*

The viability of SH-SY5Y cells decreased after being subjected to OGD/R, and then significantly increased after AAPB treatment (Fig. 5A). AAPB significantly up-regulated the levels of NO in OGD/R treated SH-SY5Y cells (Fig. 5B, C). Additionally, AAPB significantly up-regulated the levels of PTEN *S*-nitrosation (Fig. 5D, E). The addition of an NO scavenger (carboxy-PTIO) reduced the *S*-nitrosation of PTEN (Fig. 5F, G).

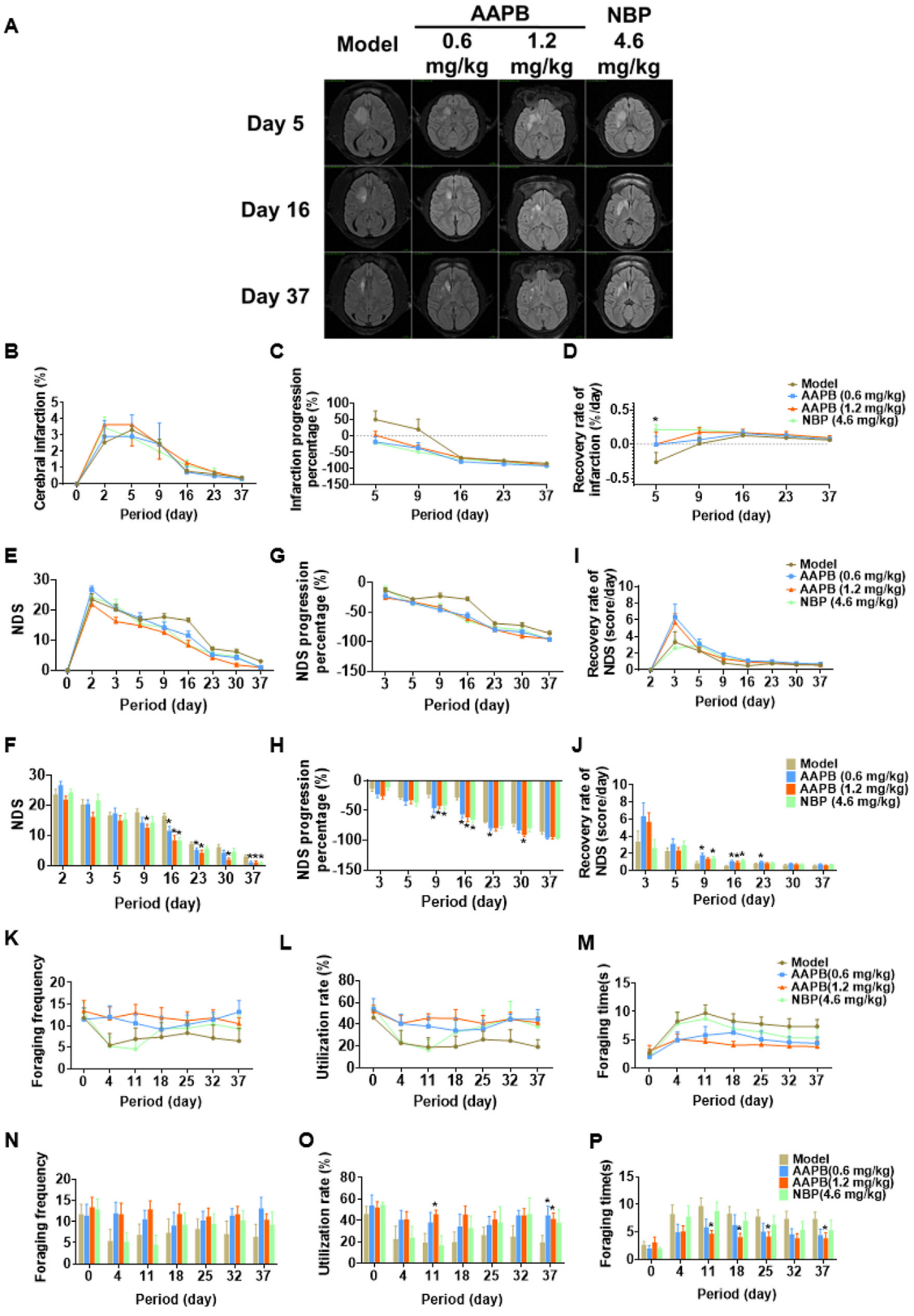

Figure 4 AAPB treatment reduced infarct volume and improved neurologic function in a rhesus monkey model of IS. (A) Typical image of MRI scan sequence (T2-Flair). (B) The extent of cerebral infarction in the rhesus monkey model of IS. (C, D) The infarction progression percentage and the recovery rate of infarction at days 5, 9, 16, 23 and 37 after modeling relative to those at day 2 after modeling. (E, F) The NDS value in the rhesus monkey model of IS. (G–J) The progression percentage and recovery rate of NDS value at days 5, 9, 16, 23 and 37 after modeling relative to those at day 2 after modeling. (K–P) The average foraging frequency, utilization rate (%) or foraging time (s) of the affected limb in the rhesus monkey model of IS. Data are mean ± SD ($n = 6$). *$P < 0.05$, compared to the model group.

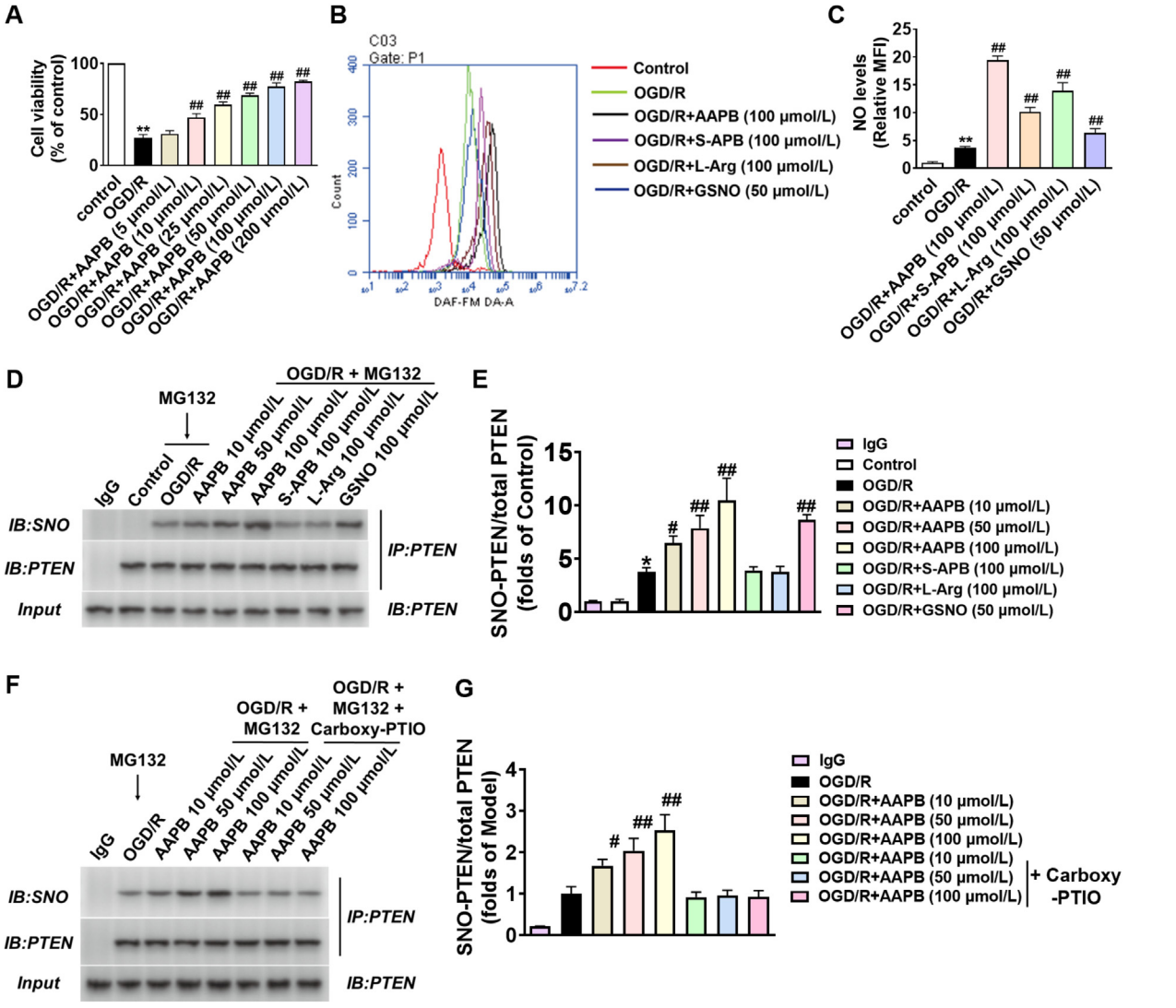

Figure 5 AAPB treatment exhibited protective activity in the OGD/R model in SH-SY5Y cell and promoted PTEN *S*-nitrosation by generating NO. (A) AAPB alleviated OGD/R-induced cytotoxicity in SH-SY5Y cells. (B, C) Different compounds released NO in SH-SY5Y cells. (D, E) Effect of different compounds on the SNO levels of PTEN in SH-SY5Y cells. (F, G) Effect of carboxy-PTIO on different compounds on the SNO levels of PTEN in SH-SY5Y cells. Data are mean ± SD ($n = 3$). $^{*}P < 0.05$ and $^{**}P < 0.01$, compared to the control group. $^{\#}P < 0.05$ and $^{\#\#}P < 0.01$, compared to the model group.

2.3.2. AAPB inhibits inflammation, oxidation and apoptosis at the cellular level

Treatment with AAPB during the recovery stage dose-dependently improved the viability of OGD/R-damaged SH-SY5Y cells, significantly decreased the contents of MDA and ROS, and increased the levels of SOD. In addition, AAPB significantly inhibited IL-6 inflammatory factor in OGD/R-induced BV-2 cells (Supporting Information Figs. S5−S7).

Treatment with AAPB significantly decreased Keap1 protein and increased p-Nrf2, HO-1, Nqo1 proteins in OGD/R-damaged SH-SY5Y cells. At the same time, the cleaved caspase-3, p-NF-κB, and Bax proteins were significantly decreased while Bcl-2 protein was increased (Supporting Information Figs. S8−S10).

2.3.3. AAPB inhibits inflammation, oxidation, and apoptosis, and promotes angiogenesis and neurogenesis in rats

AAPB reduced the levels of pro-inflammatory cytokines IL-1β, IL-6, TNF-α, IFN-γ, and IL-12p70 in infarcted cerebral tissue of animals, and the levels of TNF-α, IFN-γ, and IL-12p70 decreased significantly, compared with those in the model group, respectively (Supporting Information Fig. S11). The number of apoptotic cells in striatal volume in AAPB group was significantly decreased, compared with that in the model group, and the survival number of striatal neurons in the damaged central nervous system was significantly increased. In addition, the average optical density of CD31 in the striatum of AAPB group was higher than that of the model group (Supporting Information Fig. S12).

2.3.4. AAPB improves blood flow in cerebral ischemic tissue in tMCAO rats

The improvement of cerebral blood flow could be observed at 30, 60, 120 min after ischemia and 30, 60, 120, 240 min after perfusion in AAPB group, superior to NBP group (Fig. 6A−C). And the improvement in AAPB group was significantly inhibited by an addition of NOS inhibitor L--NAME (Fig. 6C). Moreover,

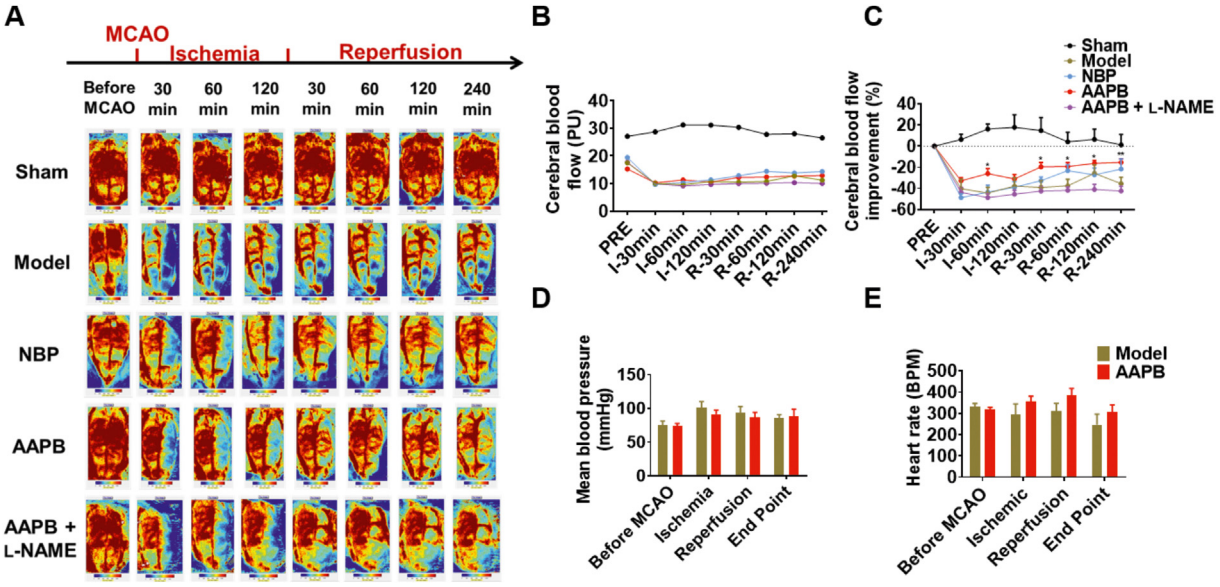

Figure 6 AAPB treatment improved blood flow in cerebral ischemic tissue in rats. (A) Laser Doppler cerebral blood flow scans of each group of animals at different time points. (B, C) Cerebral blood flow in the left cerebral hemisphere and its progression percentage in each group of animals. (D, E) Changes in mean arterial blood pressure and heart rate in the abdominal aorta at indicated time points. Data are mean ± SD ($n = 8$). *$P < 0.05$ and **$P < 0.01$, compared to AAPB + L-NAME group.

AAPB had no significant effects on mean arterial pressure and heart rate of animals at each time point (Fig. 6D, E).

2.4. *AAPB possesses good pharmacokinetic properties*

2.4.1. *Absorption*

2.4.1.1. In SD rats. After a single intravenous injection of AAPB (1.25, 5 or 20 mg/kg) to the rats, the *S*-APB system exposure level increases with the dose. The mean $t_{1/2}$ values were 5.2, 4.5, and 3.5 h, and the mean $t_{1/2}$ values (0.01667−1 h) were 0.13, 0.15, and 0.16 h, respectively, indicating that *S*-APB was cleared quickly from whole blood with a rapid decreasing trend in 1 h after administration. However, most of the concentrations increased significantly in 2−12 h after administration and then slowly eliminated. There was no significant gender difference in *S*-APB system exposure level and in other major pharmacokinetic parameters. And *S*-APB did not accumulate significantly after 7 consecutive days of administration in rats (Supporting Information Table S4).

2.4.1.2. In beagle dogs. The dogs were intravenously injected with AAPB (0.5, 1.5 or 5 mg/kg). *S*-APB was quickly cleared from the whole blood of the dogs, showing rapid distribution and elimination within 1 h after administration. There was no significant gender difference in *S*-APB system exposure in the whole blood or other major pharmacokinetic parameters. *S*-APB was exposed to a steady state after multiple doses of AAPB, without obvious accumulation after the last dose (Supporting Information Table S5).

2.4.2. *Distribution*

2.4.2.1. Plasma protein binding. At 1, 10 and 100 μg/mL, the binding rates of AAPB with the plasma protein were 90.0%, 87.6% and 83.3% for ICR mice, 90.3%, 96.3%, and 95.0% for SD rat, 90.3%, 89.1% and 84.9% for beagle dog, 90.3%, 89.7%, and 85.5% for rhesus monkey, and 97.8%, 96.7% and 94.7% for human, respectively (Supporting Information Table S6).

2.4.2.2. Tissue distribution. After a single intravenous injection of AAPB (5 mg/kg) in SD rats, *S*-APB was rapidly distributed and then quickly cleared from the tissues of the whole body. The distribution of *S*-APB was highest in whole blood, liver and kidney, followed by uterus, ovary, heart, lung and small intestine, and lower in testis, fat and brain. The *S*-APB concentration in all tissues and whole blood showed a decreasing trend with the prolonging of time. *S*-APB could be detected at a lower concentration in the brain, and there was no significant gender difference in most tissues and whole blood (Supporting Information Table S7).

2.4.3. *Metabolism*

2.4.3.1. Stablity in liver microsomes. The elimination $t_{1/2}$ values of AAPB in liver microsomes of human (phase I), human (phases I and II), cynomolgus monkey (phases I and II), beagle dog (phases I and II), SD rat (phases I and II) and CD1 mouse (phases I and II) were all greater than 120 min, respectively (Supporting Information Table S8).

2.4.3.2. Stablity in hepatocytes. The elimination $T_{1/2}$ values of AAPB in the primary hepatocytes of human, cynomolgus monkey, beagle dog, SD rat and CD1 mouse were all greater than 120 min, and the *in vitro* clearance rate (CL_{int}) is < 14.7, <22.5, <39.7, <27.0 and <68.2 mL/min/kg, respectively (Supporting Information Table S9).

2.4.3.3. Identification and relative quantification of AAPB metabolites. Major metabolites of AAPB, including *S*-APB and its products of oxidation, dehydrogenation, hydrolysis, binding of glucuronic acid, and/or oxidation plus glucuronic acid conjugates

(Supporting Information Figs. S13−S15) under different metabolic conditions were studied and their relative quantification was carried out.

2.4.3.3.1. In liver microsomes. In human liver microsomes, *S*-APB and three metabolites (M1−M3) were identified. *S*-APB and M3 occurred with relative abundances of 85.7% and 12.8%, respectively, and the other metabolites (M1 and M2) with relative abundances of less than 5.0% were observed. In monkey liver microsomes, *S*-APB at 82.7% and M3 at 17.3% were detected. In dog liver microsomes, *S*-APB at 84.8% and M3 at 15.2% were identified. In rat liver microsomes, *S*-APB at 90.7% and M3 at 9.3% were detected. And in mouse liver microsomes, *S*-APB and M3 at 82.0% and 18.0% were observed, respectively (Fig. S13).

2.4.3.3.2. In hepatocytes. After incubating with hepatocytes for 120 min, in human hepatocytes, *S*-APB and 7 metabolites (M3−M9) were detected, among which the relative abundances of *S*-APB and M8 were 86.05% and 7.55%, and the relative abundances of other metabolites were less than 5.00%. *S*-APB and 9 metabolites (M1−M9) were detected in the hepatocytes of cynomolgus monkey, the relative abundances of *S*-APB and M8 were 50.34% and 38.31%, and the relative abundances of other metabolites were less than 5.00%. In the hepatocytes of beagle dogs, *S*-APB and three metabolites (M7−M9) were detected, the relative abundances of *S*-APB and M8 were 70.02% and 24.86%, and the relative abundances of other metabolites were less than 5.00%. In the hepatocytes of SD rats, *S*-APB and 7 metabolites (M1−M4 and M7−M9) were detected, the relative abundances of *S*-APB and M8 were 82.97% and 14.95%, and the relative abundances of other metabolites were less than 5.00%. In the hepatocytes of CD1 mouse, *S*-APB and 5 metabolites (M2, M4 and M7−M9) were detected, the relative abundances of *S*-APB and M8 was 87.62% and 7.29%, and the relative abundances of other metabolites were less than 5.00%, respectively (Fig. S14).

2.4.3.3.3. In in vivo. A total of 12 metabolites (M1a, M3, M4, M6a, M6b, M7a, or M8−M13) of *S*-APB were detected and relatively quantified in whole blood, urine, stool, or bile samples from SD rats (Fig. S15).

S-APB and M8 were detected in whole blood of female SD rats, and the relative abundances of *S*-APB and M8 were 88.64% and 11.36%. *S*-APB and two metabolites (M4 and M8) were detected in whole blood of male SD rats, the relative abundances of *S*-APB and M8 were 88.47% and 11.17%, and the relative abundance of M4 was less than 1.00%.

In the urine of female SD rats, *S*-APB and five metabolites (M3, M4, M7a, M8 and M9) were detected, the relative abundances of *S*-APB, M4 and M8 were 3.91%, 2.29% and 93.80%, respectively, and other metabolites were detected but not integrated. *S*-APB and five metabolites (M3, M4, M7a, M8, and M9) were detected in the urine of male SD rats, and the relative abundances of *S*-APB, M4 and M8 were 2.99%, 6.65% and 90.36%, respectively, while other metabolites were detected but not integrated. Only *S*-APB was detected in feces of male or female SD rats.

S-APB and 12 metabolites (M1a, M3, M4, M6a, M6b, M7a and M8−M13) were detected in the bile of female SD rats, and the relative abundances of *S*-APB, M4, M6a, M8−M9 (combined), M10−M11 (combined) and M13 were 2.27%, 2.19%, 2.99%, 78.23%, 10.42% and 1.23%, respectively. The relative abundances of other metabolites were all less than 1.00%. *S*-APB and 11 metabolites (M1a, M3, M6a, M6b, M7a and M8-M13) were detected in the bile of male SD rats, and the relative abundances of *S*-APB, M1a, M3, M6a, M8-M9 (combined) and M10−M11 (combined) were 2.41%, 4.25%, 1.62%, 1.23%, 85.24% and 3.86%, respectively. The relative abundances of other metabolites were all less than 1.00%.

2.4.3.4. Metabolic characteristics in the presence of major CYP enzyme subtypes. There was no obvious metabolism of AAPB in human liver microsomal and recombinant CYP enzyme systems 90 min after incubation. In the human liver microsomal system, all CYP enzyme inhibitors had no obvious inhibitory effects on AAPB metabolism. There was no obvious metabolism of AAPB in the recombinant enzyme system (Supporting Information Tables 10 and 11).

2.4.4. Excretion

After a single intravenous injection of AAPB (5 mg/kg) in SD rats, the total fecal and urinary excretion of *S*-APB accounted for 5.070% of the administered amount within 96 h after administration, of which fecal excretion accounted for 1.084% and urine excretion accounted for 3.984%. The amount of *S*-APB excreted through bile in SD rats accounted for 1% of the dose within 72 h after administration (Supporting Information Table S12).

2.4.5. Drug−drug interactions

AAPB at 0.068−50 μmol/L did not inhibit CYP450 enzymes (CYP1A2, CYP2B6, CYP2C8, CYP2C9, CYP2C19, CYP2D6, CYP3A4 or CYP3A4 (Supporting Information Table S13), and at 0.1 or 1 μmol/L did not induce CYP450 enzymes (CYP1A2, CYP3A4, or CYP2B6) (Supporting Information Table S14).

AAPB at 0.08−50 μmol/L did not inhibit efflux transporter *ABC* (MDR1 or BCRP) (Supporting Information Table S15), and at 1 or 10 μmol/L did not act as a substrate of MDR1 or BCRP (Supporting Information Tables 16 and 17).

AAPB at 0.1, 1, 3, 10 or 50 μmol/L did not inhibit substrate uptake of uptake transporter *SLC* (OATP1B1, OATP1B3, OAT3, OCT2, MATE1 or MATE2-K) (Supporting Information Table S18), and at 1, 10 or 50 μmol/L did not act as a substrate of OATP1B1, OATP1B3, OAT1, OAT3, OCT2, MATE1 or MATE2-K (Supporting Information Table S19).

2.5. AAPB has relatively high safety

The IC_{50} of AAPB on hERG was greater than 100 μmol/L, and the neurobehavior of the rats was not affected by AAPB at 50 or 150 mg/kg in functional observation battery (FOB) test, suggesting that AAPB treatment does not inhibit hERG potassium ion channel, and AAPB at high doses functions normally on neurobehavior of rats.

AAPB at 50 or 150 mg/kg had no significant effects on the respiratory function in the awake and unbound SD rats, and at 15 mg/kg had no effects on blood pressure in awake and unrestrained beagle dogs and no effects on II-lead ECG of the dogs. These results suggest that AAPB treatment is relatively safe in the respiratory and cardiovascular systems of SD rats or beagle dogs.

The maximum tolerated dose (MTD) (1000 and 800 mg/kg) and the no observed adverse effect level (NOAEL) (400 and 150 mg/kg) of AAPB were observed in the repeated dose toxicity tests of SD rats and beagle dogs, respectively, suggesting that AAPB treatment is relatively safe in the single and repeated dose toxicity tests of SD rats and beagle dogs, respectively.

The NOAELs of parental male mice or their fertility as well as of parental female mice or their fertility or early embryonic

Table 1 The therapeutic window of AAPB in different animals.

Parameter	Animal	Minimum toxic dose (mg/kg)	Safety index (SI)
Single dose toxicity	SD rats	MTD: 1000	1000/1.2 = 833.4
	Beagle dogs	MTD: 800	800/0.36 = 2222.2
Repeated dose toxicity	SD rats	NOAEL: 400	400/1.2 = 333.3
	Beagle dogs	NOAEL: 150	150/0.36 = 416.7
Reproductive toxicity	SD rats	NOAEL: 200	200/1.2 = 166.7

development were 200 mg/kg, respectively, suggesting that reproductive toxicity test results of AAPB are negative.

The MTD of single dosing and NOAEL of repeated dosing in rats and dogs, and the NOAEL of repeated dosing in phase I reproduction of rats were several hundred times larger than the corresponding effective dose, respectively (Table 1), suggesting that the therapeutic window of AAPB is large in different animals.

And the results in the genetic toxicity (Ames, chromosome aberration and bone marrow micronucleus) as well as local tolerance (hemolysis and active systemic allergy) tests of AAPB were negative.

3. Materials and methods

3.1. Study design

This preclinical study aimed to identify a potent and safe anti-ischemic stroke candidate drug with dual actions of neuroprotection and blood flow improvement. We designed and synthesized a novel anti-IS compound based on the NVU concept and employing a design strategy of drug with multi-target action, meanwhile, performed a series of investigations in terms of effectiveness, mechanism of action, pharmacokinetics, safety, and so on, following druggability requirements.

All biological assays were performed with technical triplicates, and with positive and negative controls, as indicated in Materials and Methods and in figure legends.

All animal experiments were conducted in adherence with the Guidelines of Welfare and Ethics for the Use of Laboratory Animals, China. The experimental protocols involving rodents were approved by the Institutional Animal Care and Use Committee (IACUC) (SYXK (SU) 2016−0011). All the procedures related to handling, care, and treatment of rhesus monkeys were performed according to the guidelines approved by the IACUC (Nos. IACUC-A2022001-P-01, IACUC-A2021029-P-02, IACUC-A2021029-P-03, IACUC-A2021097-P-02, and IACUC-A2021097-P-03). The experiments were performed in accordance with the approved guidelines.

3.2. Synthesis of AAPB

The synthetic scheme for AAPB is depicted in Supporting Information Scheme S1. AAPB can be obtained from *o*-carboxybenzaldehyde by a five-step reaction sequence of cyclization, hydrolysis, chiral resolution, esterification, and salification. The detailed materials and methods can be found in the Supporting Information (Materials and Methods). The accurate configuration of the compound was validated through various analytical techniques including infrared spectroscopy (IR), high-resolution mass spectrum (HRMS), ^{1}H and ^{13}C nuclear magnetic resonance (NMR) spectroscopies, as well as X-ray single crystal diffraction analysis (Supporting Information Fig. S1).

3.3. Evaluation of pharmacodynamics

3.3.1. In a rat model of acute ischemic stroke

One hundred male SD rats were divided into seven groups of sham, model, positive drug NBP (10 mg/kg), AAPB low- (0.625 mg/kg), medium- (1.25 mg/kg), medium high- (2.5 mg/kg) and high-dose (5 mg/kg), respectively. Ten rats were assigned to the sham group and 15 rats to the other groups. The middle cerebral artery occlusion (MCAO) model of SD rats was established after the middle cerebral artery was blocked by the thread plug for 120 min and then the thread plug was pulled out for reperfusion. Each group was injected with the corresponding dose of NBP and AAPB through the tail vein immediately after reperfusion on the day of surgery (within 10 min), and then the drug intervention was performed once a day, with a total of three administration times. Triphenyltetrazolium chloride (TTC) staining was performed on the brain tissues of the animals 24 h after the end of administration to calculate the extent of cerebral infarction, and body weight monitoring and NSS were performed on the animals at days 1 and 3 after the operation, respectively. The effects of AAPB on acute IS in rats were comprehensively evaluated by the changes of cerebral infarction volume, neurofunction, and body weight.

3.3.2. In a rat model of chronic ischemic stroke

A total of eighty-seven SD rats were divided into six groups, including sham, model, NBP (5.0 mg/kg), AAPB low- (2.5 mg/kg), medium- (5.0 mg/kg), and high-dose (10 mg/kg) groups. There were 12 rats in the sham group and 15 rats in the other groups. The MCAO model of SD rats was established as mentioned above. Each group was injected with the corresponding dose of NBP and AAPB through the tail vein immediately after reperfusion on the day of operation (within 10 min), and then the drug intervention was performed once a day for 14 consecutive days. At 24 h after the end of administration, the survival of animals in each group was counted and the cerebral infarction extent was calculated by TTC staining. Meanwhile, animal weight was monitored every 2 days after operation, NSS was performed at days 1 and 7 after operation, and grid test was performed at days 7 and 14 after operation, respectively. The effects of tested compounds on chronic ischemic stroke in rats were evaluated by the changes in cerebral infarction volume, neurological function, body weight change, and animal survival.

3.3.3. Therapeutic time window in a rat model of acute ischemic stroke

One hundred and eight male SD rats were divided into eight groups of sham, model, and administration at ischemia for 1, 2, 4, 6, 8, and 24 h, respectively. And 10 rats were assigned to the sham group, and 14 rats to the other groups. The MCAO model of SD rats was established as mentioned above. The rats in administration groups received the first drug intervention by injecting 1.25 mg/kg of AAPB through the tail vein at 1, 2, 4, 6, 8, and 24 h after ischemia, respectively, and were then administered once at 24 and 48 h after surgery, with a total of three administration times

(only two times in the group at 24 h after ischemia). TTC staining was performed on the brain tissues of the animals 24 h after the end of administration to determine the volume of cerebral infarction, and body weight monitoring and NSS were performed on the animals at days 1 and 3 after operation, respectively. The therapeutic time window of AAPB for the treatment of IS was comprehensively evaluated by the changes in the cerebral infarction volume, neurological function, and body weight.

3.3.4. *In a rat model of permanent ischemic stroke*

Eighty male SD rats were divided into six groups of sham, model, NBP (10 mg/kg), and AAPB (0.625, 1.25 and 2.5 mg/kg). Ten rats were assigned to the sham group and fourteen rats to the other groups. The model of permanent cerebral ischemic stroke in rats was established by permanently blocking the middle cerebral artery with thread plugs. All administration groups were injected with corresponding doses of NBP or AAPB through the tail vein at 1 h after ischemia, and were administered once at 24 h and once at 48 h after surgery, for a total of three times. TTC staining was performed on the brain tissue of the animals 24 h after the end of administration to calculate the extent of cerebral infarction, and body weight monitoring and NSS were performed on the animals at days 1 and 3 after operation, respectively. The effect of AAPB on permanent ischemic stroke in rats was comprehensively evaluated by the changes of cerebral infarction extent, neurological function and body weight.

3.3.5. *In a rhesus monkey model of ischemic stroke*

Twenty-four male rhesus monkeys were divided into four groups of models ($n = 7$, one died after modeling, $n = 6$ at the time of statistics), NBP (4.6 mg/kg, $n = 5$), and AAPB low- (0.6 mg/kg, $n = 6$) and high-dose (1.2 mg/kg, $n = 6$). The IS model of the rhesus monkey was established by reperfusion after 2 h occlusion of the right middle cerebral artery *via* minimally invasive intervention. The animals were injected intravenously with a corresponding dose of NBP or AAPB immediately after ischemia-reperfusion and then administered once a day for 28 consecutive days. MRI was performed before surgery and at days 2, 5, 9, 16, 23, and 37 after modeling to examine cerebral infarction and calculate the extent, progression percentage, and recovery rate of cerebral infarction. NDS was performed before surgery and at days 2, 3, 5, 9, 16, 23, 30, and 37 after modeling, and the progression percentage and recovery rate of NDS were calculated, respectively. The foraging skills of the affected limb (left upper limb) were tested once before surgery and at days 4, 11, 18, 25, 32, and 37 after modeling, and the foraging frequency, utilization rate, and foraging time of the affected limb were recorded, respectively. Meanwhile, the effects of AAPB on IS in rhesus monkeys were evaluated comprehensively by monitoring the changes in animal body weight, body temperature, and general state.

3.4. *Detection of NO production and PTEN nitrosation*

3.4.1. *Detection of NO production*

The SH-SY5Y cells were divided into groups of normal (control), oxygen-glucose deprivation and recovery (OGD/R), OGD/R + AAPB (5, 10, 25, 50, 100 or 200 μmol/L), OGD/R + *S*-APB (100 μmol/L), OGD/R + L-Arg (100 μmol/L), OGD/R + L-Arg (100 μmol/L), and OGD/R + GSNO (50 μmol/L). The CCK-8 kit was used to detect the effect of each group on the viability of SH-SY5Y cells, and the DAF-FMDA probe was used to examine the levels of NO produced in SH-SY5Y cells.

3.4.2. *Detection of PTEN S-nitrosation*

The SH-SY5Y cells were divided into the following groups: normal control + MG-132, OGDR + MG-132, OGD/R + AAPB + MG-132, OGD/R + *S*-APB + MG-132, OGD/R + L-Arg + MG-132, and OGD/R + GSNO + MG-132. After OGD/R modeling, in the presence (only for AAPB group) or absence (for AAPB and other groups) of an NO scavenger, carboxy-PTIO, the cells were incubated for 1 h, and then the tested compounds were added, and incubated for 12 h. Meanwhile, MG-132 (5 μmol/L) was added to the culture medium during the culture process. Western blot and Co-IP techniques were used to examine the effects of the tested compounds on the PTEN *S*-nitrosation.

3.5. *Inhibition of inflammation, oxidation, and apoptosis at the cellular level*

The SH-SY5Y cells in the logarithmic growth phase with sugar-free serum-free medium were placed in a three-gas incubator ($O_2 \leq 0.2\%$) for 4 h of hypoxic modeling. Then, glucose and sodium pyruvate solution were added to the supernatant of the cell culture and the cells were placed in a normal incubator for 24 h to establish the OGD/R model of SH-SY5Y cells. AAPB (5, 10, 25, 50, 100, or 200 μmol/L) was added to the cells during recovery. The effect of AAPB on the viability of OGD/R damaged cells was detected by CCK-8 kit at 24 h after recovery of oxygen-glucose, *i.e.*, 24 h after administration. ROS, MDA, and SOD kits were used to detect the effect of AAPB on oxidative stress damage, and flow cytometry was employed to detect the effect of AAPB on apoptosis.

The OGD/R model of BV-2 cells was established in the same way as that of SH-SY5Y cells. The effect of AAPB on the level of inflammation was examined in the BV-2 cells after recovery of oxygen-glucose by kits of TNF-α and IL-6 at 24 h after the administration of AAPB, respectively. For the investigation of the signaling pathway, 100 μmol/L of AAPB was administered to the SH-SY5Y cells during recovery 4 h after OGD. The cells were collected for protein extraction at 6 h after AAPB administration, and Western blot assay was performed to examine the effects of AAPB on the signaling pathways of apoptotic caspase-3 and oxidative stress Nrf2, respectively.

The BV-2 cells were modeled and administered by the same method as SH-SY5Y cells, and Western blot assay was performed to determine the effect of AAPB on the inflammatory NF-κB signaling pathway in BV-2 cells.

3.6. *Inhibition of inflammation, oxidation, apoptosis and promotion of angiogenesis and neurogenesis in rats*

Thirty-four male SD rats were divided into three groups sham, model, and AAPB (1.25 mg/kg). There were 10 rats in the sham group and 12 rats in the other groups. The transient MCAO (tMCAO) model was established as mentioned above. The treatment group was injected with the corresponding dose of AAPB through the tail vein immediately after the reperfusion on the day of surgery (within 10 min), and then the surviving animals were given AAPB once a day, a total of 7 days. The NSS of AAPB-treated animals were evaluated at days 1, 4, and 7 after surgery, and the infarct side brain tissue was selected from 5 animals in each group to detect inflammatory factors and oxidative stress related indexes at day 1 after surgery, respectively. At the end of the experiment, pathological sections of cerebral tissues of the infarct side cortex and striatum were prepared from the remaining animals, and apoptosis, angiogenesis, and survival of glial cells

and neurons were detected by immunohistochemistry. The neuroprotective mechanism of AAPB in the rat ischemia-reperfusion model was comprehensively evaluated by the above indicators.

3.7. *Improvement of blood flow in cerebral ischemic tissue in rats*

Forty-eight male SD rats were divided into six groups sham, sham + AAPB (10 mg/kg), model, *S*-NBP (10 mg/kg), AAPB (10 mg/kg) + L-NAME (20 mg/kg), and AAPB (10 mg/kg), with 8 rats in each group. The model of cerebral acute ischemia induced by left middle artery blockage was established by means of the thread plug method. At 2 h after ischemia, the thread plug was removed and the left middle cerebral artery was re-opened to achieve cerebral blood flow reperfusion. The animals in the sham group were exposed only to the left internal carotid artery without insertion of the thread plug. The tested compounds were administered *via* the tail vein immediately after the model was established. The cerebral blood flow on the skull surface of the brain of the rats was evaluated by laser Doppler flow scanner at 30 min before the model, 30, 60, 120 min after ischemia, and 30, 60, 120, 240 min after reperfusion, respectively. Abdominal aortic blood pressure and heart rate were measured in the model group and AAPB group before the modeling, during ischemia, during reperfusion, and at the endpoint of the experiment, respectively.

3.8. *Statistical analysis*

The examination of data following a normal distribution was conducted using parametric tests, such as unpaired two-tailed Student's *t*-tests and one-way ANOVA, followed by Tukey's or Šidák's *post hoc* analysis. For data that did not adhere to a normal distribution, nonparametric tests such as the Mann−Whitney test or Kruskal−Wallis test, followed by Dunn's multiple comparisons tests, were employed. The data is expressed as means ± standard deviation (SD). Statistical analyses were conducted using GraphPad Prism 9 software unless otherwise specified. Statistical significance was determined by *P*-values less than 0.05.

4. Discussion

Presently, rt-PA is the only drug approved by FDA for the treatment of acute IS in the US. However, rt-PA is simply suitable for a minority of stroke patients[37,38], due to a narrow therapeutic time window and a tendency to generate bleeding side effects[2,3], as well as to the low recanalization rate (12%) for IS patients with large vessel occlusion[39].

For several decades, a large variety of drugs/agents have been investigated to protect neurons against IS, unfortunately, most of which seem promising in the preclinical studies but failed to prove neuroprotection in the clinical trials[40-47], and so far there are no approved neuroprotective drugs fighting IS except NBP and Eda[13].

Given that many drugs/agents with the significant neuroprotection but no blood flow improvement was unsuccessful against IS in clinic, and that the thrombolytic drugs like rt-PA only improving blood flow without neuroprotection generally possess therapeutic limitation and risk of hemorrhagic transformation[48], as well as that brain vascular recanalization in combination with neuroprotective drugs/agents may improve therapeutic results[6-12], we assumed that an agent with dual effects of neuroprotection and cerebral blood flow improvement may become a promising anti-IS candidate drug, and thus constructed and biologically evaluated the novel compound AAPB to testify the hypothesis.

Firstly, AAPB exerted significant inhibitory effects on ADP- or AA-induced platelet aggregation and on coagulation, and its antithrombotic activity in a rat arteriovenous shunt thrombosis model was superior to ASP, *S*-NBP and PHPB, respectively.

Subsequently, AAPB substantially inhibited cerebral infarction and neurological deficit in tMCAO rats, more active than NBP, and at 8 h post stroke still had a significant neuroprotective effect. Moreover, AAPB obviously improved blood flow in the rat brain ischemic tissues without affecting blood pressure and heart rate, better than NBP.

In the present, only a small percentage of IS patients can receive the recanalization therapy, permanent ischemia without reperfusion remains a big challenge post IS. Notably, AAPB could significantly reduce the cerebral infarction volume of permanent MCAO (pMCAO) rats, whereas NBP had no obvious improvement on that, meanwhile AAPB improved the neurological function, faster than NBP, probably because the cerebral blood flow was improved by action of NO produced from AAPB, at least in part. This result suggests the potential efficacy of AAPB in the future for treating IS patients illegible to undergo thrombolysis or thrombectomy.

For a long time, most of anti-stroke researches focused on the neuron injuries in the acute phase of IS, and paid a little attention to the secondary damage in the recovery period of IS[49]. Importantly, from days 18 to 37 after modeling, the average foraging frequencies and utilization rates of the affected limb of rhesus monkeys in AAPB low- or high-dose group were not significantly decreased, compared with those before modeling, and were significantly higher than those in the model or NBP group at corresponding time points. And the foraging time of AAPB low- or high-dose group at each time point was significantly decreased, compared with that in the model or NBP group. These results suggest that AAPB may be possible to greatly improve the patients' quality of life in the recovery period of IS.

S-Nitrosation is one of the main mechanisms for the signaling and biological activities of NO, which is same important as phosphorylation, acetylation or other post-translational modification of protein[50-54].

AAPB up-regulated the levels of PTEN *S*-nitrosation in the rat cerebral ischemic zone and the NO scavenger significantly mitigated *S*-nitrosation, attenuating the protective activity of AAPB, suggesting that the low amounts of NO generated from L-Arg in AAPB may *S*-nitrosate PTEN and inhibit its activity, thus activate PI3k/Akt pathway, playing the neuroprotective role. Moreover, AAPB also NO-dependently improved the cerebral blood flow in the rat brain ischemic tissues.

Since relatively high levels of endogenous L-Arg may cause serious interference with the identification of the L-Arg metabolized from AAPB, we synthesize N^{15}- and H^{2}-labelled AAPB by saltification of *S*-APB with the labelled L-Arg. Expectedly, the metabolites generated from the labelled AAPB included the labelled L-Arg besides *S*-APB in the rat brain tissue. In this way, the L-Arg metabolized from AAPB was confirmed. Possibly, the L-Arg may enter the brain from blood circulation *via* the cationic amino acid transporter on the blood−brain barrier[55].

Interestingly, AAPB displayed high protein binding rate, that may result in a continuous release of AAPB in the blood, maintaining a stable drug concentration to display a good therapeutic effect.

Under the experimental conditions, AAPB had no inhibitive or inductive effect on the CYP450 enzyme system, as well as no

inhibitive or inductive or substrate characteristic on the efflux *ABC* transporters and the uptake transporter *SLC*.

Furthermore, AAPB showed exceptional *in vitro* and *in vivo* safety profiles, with a big therapeutic window or safe index, and may be relatively safe for the treatment of IS patients in the clinical tries.

It should be stressed that an ideal positive control compound in new drug research generally meets the following criteria. Firstly, it should be authoritative, preferably a marketed or clinically approved drug, or a safe and effective agent cited or published in the high-quality scientific journals. Secondly, it should share similar chemical structure, mechanism of action and/or indications with that of the compounds under investigation. Finally, it should be administered through the same route as the tested compounds.

NBP is an anti-IS drug first launched in China in 2004 and until now still widely used for the treatment of IS. NBP possesses multi-target effects, involving inhibition of neuronal apoptosis, improvement of mitochondrial function and cerebral blood flow, as well as anti-oxidation and anti-inflammation, etc[56]. AAPB is an ester derivative of PHPB which generated from the ring-opening of the lactone in NBP with an anti-IS activity comparable to NBP but better physicochemical and pharmacokinetic properties[31-34]. PHPB is now in II−III phase of clinical trials fighting the acute IS. Hence, for the sake of objectivity, persuasion, continuity and consistency of research, we chose only NBP as the positive control to systematically and comprehensively evaluate the anti-IS efficacy of AAPB in all *in vivo* experiments involving SD rats and rhesus monkeys.

Our findings are in line with the previously proposed scientific hypothesis, and AAPB has now entered the phase I of clinical trials in China.

5. Conclusions

In conclusion, by combining neuroprotection with enhanced cerebral blood flow, the efficacy of AAPB outperforms the current neuroprotective drugs like NBP. Furthermore, AAPB's favorable pharmacokinetics, little interaction with key drug-metabolizing enzymes, and outstanding safety profile may position it as a promising drug in the future for the treatment of IS patients, especially those ineligible for thrombolysis or thrombectomy.

Acknowledgments

This work was supported by grants from the National Natural Science Foundation of China (Nos. 82273780, 82173681 and 82104004), the Natural Science Foundation of Xinjiang Uygur Autonomous Region (2022D01D38, China), the open projects of State Key Laboratory of Natural Medicines (No. SKLNMZZ202213, China) and the State Key Laboratory of Pathogenesis, Prevention, and Treatment of High Incidence Diseases in Central Asia Fund (SKL-HIDCA-2021-1, China), and the Fundamental Research Funds for the Central Universities of China Pharmaceutical University (No. 2632023TD04).

Author contributions

Jianbing Wu: Writing − review & editing, Methodology, Investigation. Duorui Ji: Writing − review & editing, Investigation. Weijie Jiao: Investigation. Jian Jia: Investigation. Jiayi Zhu: Investigation. Taijun Hang: Writing − review & editing, Investigation. Xijing Chen: Methodology, Investigation. Yang Ding: Methodology, Investigation. Yuwen Xu: Methodology. Xinglong Chang: Methodology, Investigation. Liang Li: Investigation. Qiu Liu: Investigation. Yumei Cao: Investigation. Yan Zhong: Investigation. Xia Sun: Investigation. Qingming Guo: Investigation. Tuanjie Wang: Investigation. Zhenzhong Wang: Methodology. Ya Ling: Methodology. Wei Xiao: Writing − review & editing, Conceptualization. Zhangjian Huang: Writing − review & editing, Conceptualization. Yihua Zhang: Writing − review & editing, Methodology, Conceptualization.

Conflicts of interest

The authors have no conflicts of interest to declare.

Appendix A. Supporting information

Supporting information to this article can be found online at https://doi.org/10.1016/j.apsb.2024.12.042.

References

1. Zerna C, Hegedus J, Hill MD. Evolving treatments for acute ischemic stroke. *Circ Res* 2016;**118**:1425−42.
2. Jung S, Gralla J, Fischer U, Mono ML, Weck A, Lüdi R, et al. Safety of endovascular treatment beyond the 6-h time window in 205 patients. *Eur J Neurol* 2013;**20**:865−71.
3. Schellinger PD, Thomalla G, Fiehler J, Köhrmann M, Molina CA, Neumann-Haefelin T, et al. MRI-based and CT-based thrombolytic therapy in acute stroke within and beyond established time windows: an analysis of 1210 patients. *Stroke* 2007;**38**:2640−5.
4. Chamorro Á, Dirnagl U, Urra X, Planas AM. Neuroprotection in acute stroke: targeting excitotoxicity, oxidative and nitrosative stress, and inflammation. *Lancet Neurol* 2016;**15**:869−81.
5. Gerschenfeld G, Muresan IP, Blanc R, Obadia M, Abrivard M, Piotin M, et al. Two paradigms for endovascular thrombectomy after intravenous thrombolysis for acute ischemic stroke. *JAMA Neurol* 2017;**74**:549−56.
6. Amaro S, Renú A, Laredo C, Castellanos M, Arenillas JF, Llull L, et al. Relevance of collaterals for the success of neuroprotective therapies in acute ischemic stroke: insights from the randomized URICO-ICTUS trial. *Cerebrovasc Dis* 2019;**47**:171−7.
7. Chen D, Yin Y, Shi J, Yang F, Wang K, Zhao F, et al. DL-3-n-butylphthalide improves cerebral hypoperfusion in patients with large cerebral atherosclerotic stenosis: a single-center, randomized, double-blind, placebo-controlled study. *BMC Neurol* 2020;**20**:212.
8. Elkind MS, Sacco RL, MacArthur RB, Fink DJ, Peerschke E, Andrews H, et al. The Neuroprotection with Statin Therapy for Acute Recovery Trial (NeuSTART): an adaptive design phase I dose-escalation study of high-dose lovastatin in acute ischemic stroke. *Int J Stroke* 2008;**3**:210−8.
9. Fraser JF, Maniskas M, Trout A, Lukins D, Parker L, Stafford WL, et al. Intra-arterial verapamil post-thrombectomy is feasible, safe, and neuroprotective in stroke. *J Cereb Blood Flow Metab* 2017;**37**:3531−43.
10. Fraser JF, Pahwa S, Maniskas M, Michas C, Martinez M, Pennypacker KR, et al. Now that the door is open: an update on ischemic stroke pharmacotherapeutics for the neurointerventionalist. *J Neurointerv Surg* 2024;**16**:425−8.
11. Zhang X, Zhong W, Ma X, Zhang X, Chen H, Wang Z, et al. Ginkgolide with intravenous alteplase thrombolysis in acute ischemic stroke improving neurological function: a multicenter, cluster-randomized trial (GIANT). *Front Pharmacol* 2021;**12**:792136.
12. Dammavalam V, Lin S, Nessa S, Daksla N, Stefanowski K, Costa A, et al. Neuroprotection during thrombectomy for acute ischemic stroke: a review of future therapies. *Int J Mol Sci* 2024;**25**:891.

13. Jia J, Jiao W, Wang G, Wu J, Huang Z, Zhang Y. Drugs/agents for the treatment of ischemic stroke: advances and perspectives. *Med Res Rev* 2023;**44**:975−1012.
14. Khoshnam SE, Winlow W, Farzaneh M, Farbood Y, Moghaddam HF. Pathogenic mechanisms following ischemic stroke. *Neurol Sci* 2017;**38**:1167−86.
15. Casas AI, Hassan AA, Larsen SJ, Gomez-Rangel V, Elbatreek M, Kleikers PWM, et al. From single drug targets to synergistic network pharmacology in ischemic stroke. *Proc Natl Acad Sci U S A* 2019;**116**:7129−36.
16. Lo EH, Dalkara T, Moskowitz MA. Mechanisms, challenges and opportunities in stroke. *Nat Rev Neurosci* 2003;**4**:399−415.
17. Moskowitz MA, Lo EH, Iadecola C. The science of stroke: mechanisms in search of treatments. *Neuron* 2010;**67**:181−98.
18. Ozaki T, Nakamura H, Kishima H. Therapeutic strategy against ischemic stroke with the concept of neurovascular unit. *Neurochem Int* 2019;**126**:246−51.
19. Hill MD, Goyal M, Menon BK, Nogueira RG, McTaggart RA, Demchuk AM, et al. Efficacy and safety of nerinetide for the treatment of acute ischaemic stroke (ESCAPE-NA1): a multicentre, double-blind, randomised controlled trial. *Lancet* 2020;**395**:878−87.
20. Montaner J, Campos M, Cristobo I, Giralt D, Díaz-Guerra M. Role of PSD-95 inhibitors in stroke and neuroprotection: a systematic review on NA-1 (Tat-NR2B9c). *Drugs Future* 2013;**38**:485−97.
21. Hong JM, Kim DS, Kim M. Hemorrhagic transformation after ischemic stroke: mechanisms and management. *Front Neurol* 2021;**12**:703258.
22. Kong L, Ma Y, Li L, Chen Y, Du G. Advances in the study of mechanism of thrombolysis-induced hemorrhagic transformation and therapeutic drugs. *Acta Pharm Sin* 2018;**53**:1467−76.
23. van Kranendonk KR, Treurniet KM, Boers AMM, Berkhemer OA, van den Berg LA, Chalos V, et al. Hemorrhagic transformation is associated with poor functional outcome in patients with acute ischemic stroke due to a large vessel occlusion. *J Neurointerv Surg* 2019;**11**:464−8.
24. Garry PS, Ezra M, Rowland MJ, Westbrook J, Pattinson KT. The role of the nitric oxide pathway in brain injury and its treatment—from bench to bedside. *Exp Neurol* 2015;**263**:235−43.
25. Khan M, Dhammu TS, Qiao F, Kumar P, Singh AK, Singh I. *S*-Nitrosoglutathione mimics the beneficial activity of endothelial nitric oxide synthase-derived nitric oxide in a mouse model of stroke. *J Stroke Cerebrovasc Dis* 2019;**28**:104470.
26. Wu J, Jia J, Ji D, Jiao W, Huang Z, Zhang Y. Advances in nitric oxide regulators for the treatment of ischemic stroke. *Eur J Med Chem* 2023;**262**:115912.
27. Wu J, Yin W, Huang Z, Zhang Y, Jia J, Cheng H, et al. Design, synthesis, and biological evaluation of organic nitrite (NO_2^-) donors as potential anticerebral ischemia agents. *J Med Chem* 2021;**64**:10919−33.
28. Fonar G, Polis B, Meirson T, Maltsev A, Elliott E, Samson AO. Intracerebroventricular administration of L-arginine improves spatial memory acquisition in triple transgenic mice *via* reduction of oxidative stress and apoptosis. *Transl Neurosci* 2018;**9**:43−53.
29. Koga Y, Akita Y, Nishioka J, Yatsuga S, Povalko N, Tanabe Y, et al. L-Arginine improves the symptoms of strokelike episodes in MELAS. *Neurology* 2005;**64**:710−2.
30. Moreira AS, Estato V, Malvar DC, Sanches GS, Gomes F, Tibirica E, et al. L-Arginine supplementation and thromboxane synthase inhibition increases cerebral blood flow in experimental cerebral malaria. *Sci Rep* 2019;**9**:13621.
31. Li J, Wang XL, Wang AP, Xu SF, Jin HT. Toxicokinetics and toxicity of potassium 2-(1-hydroxypentyl)-benzoate in beagle dogs. *J Asian Nat Prod Res* 2017;**19**:388−401.
32. Li J, Xu SF, Peng Y, Feng N, Wang L, Wang XL. Conversion and pharmacokinetics profiles of a novel pro-drug of 3-*n*-butylphthalide, potassium 2-(1-hydroxypentyl)-benzoate, in rats and dogs. *Acta Pharmacol Sin* 2018;**39**:275−85.
33. Liu D, Zhang M, Rong X, Li J, Wang X. Potassium 2-(1-hydroxypentyl)-benzoate attenuates neuronal apoptosis in neuron-astrocyte co-culture system through neurotrophy and neuro-inflammation pathway. *Acta Pharm Sin B* 2017;**7**:554−63.
34. Zhao C, Hou W, Lei H, Huang L, Wang S, Cui D, et al. Potassium 2-(L-hydroxypentyl)-benzoate attenuates neuroinflammatory responses and upregulates heme oxygenase-1 in systemic lipopolysaccharide-induced inflammation in mice. *Acta Pharm Sin B* 2017;**7**:470−8.
35. Miner J, Hoffhines A. The discovery of aspirin's antithrombotic effects. *Tex Heart Inst J* 2007;**34**:179−86.
36. Richman IB, Owens DK. Aspirin for primary prevention. *Med Clin North Am* 2017;**101**:713−24.
37. Campbell BCV, Khatri P. Stroke. *Lancet* 2020;**396**:129−42.
38. Stinear CM, Lang CE, Zeiler S, Byblow WD. Advances and challenges in stroke rehabilitation. *Lancet Neurol* 2020;**19**:348−60.
39. Lee MH, Im SH, Jo KW, Yoo DS. Recanalization rate and clinical outcomes of intravenous tissue plasminogen activator administration for large vessel occlusion stroke patients. *J Korean Neurosurg Soc* 2023;**66**:144−54.
40. Dawson LA, Djali S, Gonzales C, Vinegra MA, Zaleska MM. Characterization of transient focal ischemia-induced increases in extracellular glutamate and aspartate in spontaneously hypertensive rats. *Brain Res Bull* 2000;**53**:767−76.
41. Gardner AJ, Menon DK. Moving to human trials for argon neuroprotection in neurological injury: a narrative review. *Br J Anaesth* 2018;**120**:453−68.
42. Kalogeris T, Baines CP, Krenz M, Korthuis RJ. Cell biology of ischemia/reperfusion injury. *Int Rev Cell Mol Biol* 2012;**298**:229−317.
43. Lai TW, Zhang S, Wang YT. Excitotoxicity and stroke: identifying novel targets for neuroprotection. *Prog Neurobiol* 2014;**115**:157−88.
44. Nolan JP, Sandroni C, Böttiger BW, Cariou A, Cronberg T, Friberg H, et al. European resuscitation council and european society of intensive care medicine guidelines 2021: post-resuscitation care. *Intensive Care Med* 2021;**47**:369−421.
45. O'Collins VE, Macleod MR, Donnan GA, Horky LL, van der Worp BH, Howells DW. 1,026 experimental treatments in acute stroke. *Ann Neurol* 2006;**59**:467−77.
46. Scheid S, Goebel U, Ulbrich F. Neuroprotection is in the air-inhaled gases on their way to the neurons. *Cells* 2023;**12**:2480.
47. Vats K, Sarmah D, Datta A, Saraf J, Kaur H, Pravalika K, et al. Intra-arterial stem cell therapy diminishes inflammasome activation after ischemic stroke: a possible role of acid sensing ion channel 1a. *J Mol Neurosci* 2021;**71**:419−26.
48. Zubair AS, Sheth KN. Hemorrhagic conversion of acute ischemic stroke. *Neurotherapeutics* 2023;**20**:705−11.
49. Qi H, Tian D, Luan F, Yang R, Zeng N. Pathophysiological changes of muscle after ischemic stroke: a secondary consequence of stroke injury. *Neural Regen Res* 2024;**19**:737−46.
50. Chen YJ, Liu YC, Liu YW, Lee YB, Huang HC, Chen YY, et al. Nitrite protects neurons against hypoxic damage through *S*-nitrosylation of caspase-6. *Antioxid Redox Signal* 2019;**31**:109−26.
51. Foster MW, McMahon TJ, Stamler JS. *S*-Nitrosylation in health and disease. *Trends Mol Med* 2003;**9**:160−8.
52. Huang Z, Fu J, Zhang Y. Nitric oxide donor-based cancer therapy: advances and prospects. *J Med Chem* 2017;**60**:7617−35.
53. Mintz J, Vedenko A, Rosete O, Shah K, Goldstein G, Hare JM, et al. Current advances of nitric oxide in cancer and anticancer therapeutics. *Vaccines (Basel)* 2021;**9**:94.
54. Ye H, Wu J, Liang Z, Zhang Y, Huang Z. Protein *S*-nitrosation: biochemistry, identification, molecular mechanisms, and therapeutic applications. *J Med Chem* 2022;**65**:5902−25.
55. Tachikawa M, Hirose S, Akanuma SI, Matsuyama R, Hosoya KI. Developmental changes of L-arginine transport at the blood−brain barrier in rats. *Microvasc Res* 2018;**117**:16−21.
56. Marco-Contelles J, Zhang Y. From seeds of apium graveolens linn to a cerebral ischemia medicine: the long journey of 3-*N*-butylphthalide. *J Med Chem* 2020;**63**:12485−510.